SCIENTIFIC REPORTS

SUBJECT AREAS:
NEURODEGENERATION
MOLECULAR NEUROSCIENCE
PROTEIN METABOLISM
BEHAVIOUR

Received
5 October 2011

Accepted
13 January 2012

Published
13 February 2012

Correspondence and requests for materials should be addressed to D.R.S. (derya.shimshek@novartis.com)

Excess α-synuclein worsens disease in mice lacking ubiquitin carboxy-terminal hydrolase L1

Derya R. Shimshek, Tatjana Schweizer, Peter Schmid & P. Herman van der Putten

Neuroscience Research, Novartis Institutes for BioMedical Research, Novartis Pharma AG, 4002 Basel, Switzerland.

Mutations in α-synuclein (αSN) and ubiquitin carboxy-terminal hydrolase L1 (UCH-L1) have been linked to familial Parkinson's disease (PD). Physical and functional interactions between these two proteins have been described. Whether they act additively *in vivo* to influence disease has remained controversial. αSN is a presynaptic protein and the major constituent of Lewy inclusions, histopathological hallmarks of PD. UCH-L1 regulates ubiquitin stability in the nervous system and its loss results in neurodegeneration in peripheral and central neurons. Here, we used genetics to show that UCH-L1-deficiency together with excess αSN worsen disease. Double mutant mice show earlier-onset motor deficits, a shorter lifespan and forebrain astrogliosis but the additive disease-worsening effects of UCH-L1-deficiency and excess αSN are not accompanied by microgliosis, ubiquitin pathology or changes in pathological αSN protein levels and species.

Parkinson's disease (PD) is a progressive neurodegenerative disorder that affects approximately 1% of the population older than 65 years of age. Disabling clinical manifestations are caused by a selective loss of dopaminergic (DA) neurons in the substantia nigra pars compacta (SNc) and include tremor, bradykinesia and stiffness. DA neuronal cell loss is accompanied by an immunopathology in DA and other neurons: eosinophilic intraneuronal inclusions referred to as either Lewy bodies (LBs) or Lewy neurites (LNs). Both are composed mainly of α-synuclein (αSN) and often also ubiquitin (Ub). Like in PD, Lewy inclusions are a defined pathological hallmark of another α-synucleinopathy disease referred to as dementia with Lewy bodies (DLB; for review see[1,2]). DLB is second after the most common neurofibrillary pathology that characterizes Alzheimer's disease (AD) and often both pathologies co-occur in the same individual. In contrast to AD pathology, Lewy pathology is not restricted to central neurons but also occurs in peripheral neurons and nerves including the gastrointestinal nervous system and cardiac nerves[3].

In recent years, hope has risen to better understand the pathophysiology of α-synucleinopathies. The evidence, that the accumulation of non-physiological levels and forms of the synaptic protein αSN plays a central role in disease pathogenesis is overwhelming[4]: (i) αSN accumulates in LBs[5–7]; (ii) specific mutations in αSN causing a single amino-acid change (A30P, A53T, E46K) as well as duplication or triplication of the wildtype αSN gene cause rare familial forms of parkinsonism[8–11]; (iii) neuronal over-expression of either wildtype or mutant human αSN in transgenic flies, rodents and non-human primates causes α-synucleinopathy[12–16]. Nonetheless, the molecular mechanisms causing a non-physiological accumulation of αSN and/or αSN-induced neuronal dysfunction and death have remained largely elusive.

The enzyme ubiquitin carboxy-terminal hydrolase L1 (UCH-L1) is primarily expressed in neurons and has been implicated in neurodegenerative diseases including PD as well as cancer[17,18]. UCH-L1 protein is abundant and widely expressed in the brain (1–2% of total protein). The enzyme has de-ubiquitylating[19,20] as well as ubiquitylating activity[21], and the protein functions to stabilize mono-ubiquitin[22]. UCH-L1 protein is found in Lewy bodies[23]. A missense mutation (I93M) in UCH-L1 (UCH-L1^{I93M}) was discovered in a German family affected by autosomal dominant familial PD[24]. Other reports linking UCH-L1 variants as risk factors for PD have remained controversial[25–27]. Mice naturally lacking UCH-L1 develop gracile axonal dystrophy (gad), exhibit an age-dependent sensory ataxic phenotype and motor paresis, manifest a dying-back axonal degeneration in sensory and motor nerve terminals and display β-synuclein (βSN) and γ-synuclein (γSN) pathology but, interestingly, lack αSN pathology[28–30]. Evidence from two additional different UCH-L1-deficient mouse mutants showed that UCH-L1 is required for maintaining the structure and function of central and peripheral synapses[31,32]. None of these mutants seems to show pathological changes in dopaminergic neurons and the extent of viral vector-mediated expression and αSN-induced cell loss in DA neurons is exacerbated in UCH-L1^{I93M}

transgenic but not in wildtype UCH-L1 (UCH-L1^{wildtype}) or gad mice[33]. All these findings seem consistent with a gain-of-toxic function of the UCH-L1^{I93M} mutant but little or no function of UCH-L1^{wildtype} or its lack in αSN-induced DA damage.

Also in line with this hypothesis are the reports that over-expression of the UCH-L1^{I93M} mutant *in vitro* causes accumulation of αSN[34] and in mice leads to DA neuronal cell loss[35]. Nonetheless, other findings suggest that also UCH-L1^{wildtype} has a role in αSN-induced neurotoxicity and αSN protein homeostasis: (i) different forms of UCH-L1 de-ubiquitinate poly-ubiquitinated αSN[36,37] or act as an αSN ubiquitin ligase[21]; (ii) UCH-L1 levels are reduced and activity is down by 40-80% because of oxidative damage in idiopathic PD, DLB and AD brains[38,39]; (iii) reducing the membrane-bound from of UCH-L1 in cell culture models of αSN toxicity reduces αSN levels and increases cell viability[40]. Here, we used mouse genetics to further elucidate a potential synergistic effect of UCH-L1-deficiency and excess αSN in disease.

Results

Excess αSN worsens disease in UCH-L1-deficient mice. To test whether excess αSN and the lack of UCH-L1 have additive effects on disease worsening or outcome, we generated via breeding double transgenic mice over-expressing wildtype mouse αSN[41] (Thy1-maSN) and lacking UCH-L1 [Deltagen (Uchl1^{tm1Dgen}; ID: MGI: 3604452)]. We studied UCH-L1-deficiency in the context of an excess of murine wildtype αSN to avoid confounds that might arise because of cross-species differences in human and mouse αSN and/or UCH-L1 function. Double Uchl1^{tm1Dgen}:Thy1-maSN transgenic mice (referred to as UCH-L1$^{-/-}$/Thy1-maSN hereafter), and their single mutant UCH-L1$^{-/-}$ and Thy1-maSN littermates were subsequently characterized with respect to weight, muscle strength (grip strength), motor coordination (rotating beam performance) and α-synucleinopathy related changes at histopathological and biochemical levels. At 2.5 months of age, wildtype control littermates and Thy1-maSN mice showed no difference in weight (Figure 1A), grip strength (Figure 1B) or rotating beam performance (Figure 1C and 1D). In contrast, at this age UCH-L1$^{-/-}$ mice showed already a slight weight-loss (Figure 1A) and motor deficits on the rotating beam (Figure 1C and 1D), a phenotype similar to that described for UCH-L1 deficient gad mice[42]. Muscle weakness in UCH-L1$^{-/-}$ mice was not yet apparent at the age of 2.5 months (Figure 1B) but very prominent at the age of 4.5 months (0.62 N ± 0.14 versus littermate controls 1.32 N ± 0.14). Heterozygous UCH-L1 deficient mice did not show these deficits (data not shown). As compared to UCH-L1$^{-/-}$ mice, 2.5 months old UCH-L1$^{-/-}$/Thy1-maSN double mutant mice showed greater deficits in both muscle strength (Figure 1B) and motor coordination (Figure 1C and 1D) whereas weight did not differ significantly (Figure 1A). At the age of 3.5 months, the general health state of double mutant mice was such, that the animals had to be

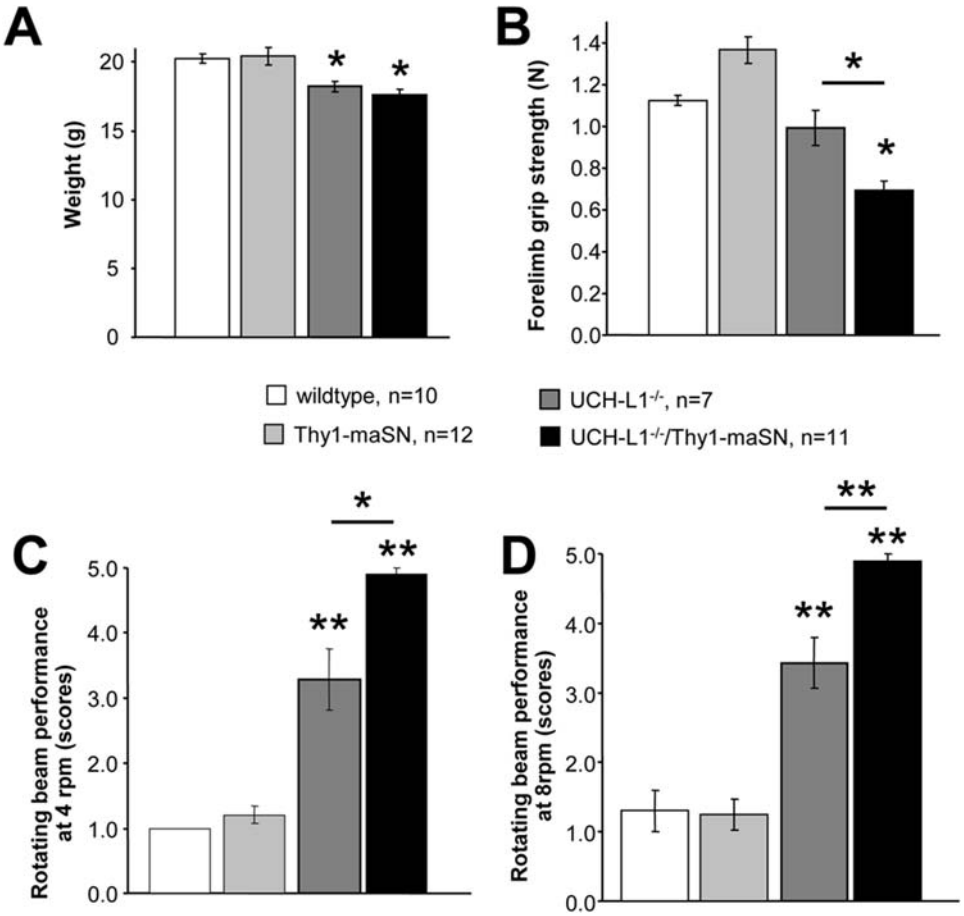

Figure 1 | Weight, muscle strength and motor behavior in UCH-L1$^{-/-}$/Thy1-maSN double transgenic mice. (A) Small weight-loss effect in UCH-L1$^{-/-}$ and UCH-L1$^{-/-}$/Thy1-maSN mice as compared to the other genotypes and wildtype mice. (B) Significant reduction in forelimb grip strength in UCH-L1$^{-/-}$/Thy1-maSN mice as compared to unchanged strengths in the other genotypes. (C) Performance of motor coordination assessed on the rotating beam at 4 rpm. (D) Performance of motor coordination assessed on the rotating beam at 8 rpm. UCH-L1$^{-/-}$/Thy1-maSN mice are more severely impaired as compared to UCH-L1$^{-/-}$ mice. Motor performance by the other genotypes was not impaired. Age of the mice: 2.5 months. Data are shown as mean ± SEM. See colour code for the different genotypes. N numbers for each genotype are indicated. *p<0.05, **p<0.01 (two-tailed, unequal variances Student's t-test).

sacrificed in agreement with local regulations for animal experimentation. It was clear that unlike their single UCH-L1$^{-/-}$ and Thy1-maSN mutant littermates, double mutant mice would never reach an age of 5–6 months or older, as described for mice lacking either only UCH-L1[42] or over-expressing mouse αSN[41]. For reference, UCH-L1$^{+/-}$/Thy1-maSN double and Thy1-maSN single mutant mice showed no significant differences in performance or health state (data not shown). Thus, disease worsening is only observed under conditions of excess murine αSN and a complete lack of UCH-L1.

UCH-L1 deficiency promotes early-onset astrogliosis in Thy1-maSN mice. Next, we determined whether UCH-L1-deficiency combined with excess wildtype αSN affected histopathological hallmarks of disease and/or pathological αSN protein levels and species. Over-expression of murine αSN resulted in increased perikaryal αSN accumulation in the cell soma as illustrated in hippocampal neurons (Figure 2). The same phenomenon occurs also in mice expressing human wildtype or A53T mutant αSN[16] but with one distinction: mice expressing murine wildtype αSN appear to have less and a more diffuse neuritic αSN staining as opposed to the overall increased intensity and often focal accumulation type αSN staining patterns observed in neurites of mice expressing human αSN forms. Stainings of littermate brains with different genotypes were always done in parallel and at the same time using identical conditions so it remains to be determined whether epitope masking or other reasons account for this phenomenon in Thy1-maSN mice. Control littermates and age-matched UCH-L1$^{-/-}$ mice did not show this transgene-specific pattern of perikaryal αSN immunolabeling in stratum pyramidale neurons. Instead, UCH-L1$^{-/-}$ mice showed a for wildtype mice typical strong αSN immunolabeling in stratum radiatum and stratum oriens and virtually no staining in cell soma (Figure 2). At age 3.5 months, Thy1-maSN single and UCH-L1$^{-/-}$/Thy1-maSN double mutants showed similar patterns of perikaryal murine αSN accumulation in hippocampal neurons (Figure 2). Therefore, the lack of UCH-L1 by itself does not provoke a perikaryal accumulation of endogenous murine αSN and in double mutants, it does not significantly alter the pattern of perikaryal αSN accumulation seen in hippocampal neurons and other brain areas including the motor cortex, the striatum and the brainstem (Figure 2).

The most prominent finding that distinguished double from single mutant mice at the age of 3.5 months was a substantial increase in astrogliosis. 4/7 double mutant mice as compared to their single mutant littermates showed massive astrogliosis, especially in the cortex and to a lesser extent in the hippocampus and the striatum (Figure 3). This was verified in immunoblots of anterior brain extracts detecting increased levels of GFAP in 3/6 UCH-L1$^{-/-}$/Thy1-maSN double mutant mice (see Supplementary Fig. S1 online). The fact that not all double mutants showed these histopathological changes at age 3.5 months is not surprising because we also observed significant heterogeneity in (i) the age at which disease-onset is phenotypically manifest in individual Thy1-maSN mice, (ii) the age-at-onset at which astro- and microgliosis occurs in the most profoundly affected brain regions such as brainstem in Thy1-maSN mice, and (iii) the age at which end-stage pathology and disease is reached (varies between 6 and 10 months). Puzzling is that other brain regions including e.g. cerebellum, brainstem, and thalamus showed no signs of astrogliosis (Figure 3 and data not shown). Also, all brain regions examined in 3.5 month old mice were devoid of enhanced ubiquitin staining, microgliosis and axon degeneration (data not shown), which all are histopathological changes present in end-stage Thy1-maSN mice[41]. In summary, excess αSN in UCH-L1-deficient mice specifically leads to an early-onset astrogliosis in forebrain regions where neurons express high levels of transgene-derived αSN.

UCH-L1 deficiency in Thy1-maSN mice does not alter the levels of monomeric, oligomeric or S129-phosphorylated αSN forms. Immunoblot analysis of the soluble protein fraction extracted from forebrain and brainstem regions of 3.5-month-old Thy1-maSN mice revealed, besides increased levels of monomeric αSN, high-molecular weight αSN forms as well as truncated species and increased levels of S129-phosphorylated αSN (Figure 4A and 4B). We have described similar soluble αSN species in mice over-expressing the human αSN(A53T) mutant[43]. The lack of UCH-L1 in the double mutant mice did not significantly change the pattern and level of αSN species seen in single Thy1-maSN mutants (Figure 4A, 4B and 4C). In addition, UCH-L1$^{-/-}$ and wildtype littermates showed indistinguishable levels and patterns of soluble αSN species (Figure 4A, 4B and 4C). Finally, genotype-specific differences were also not observed following immunoblotting the insoluble αSN (pellet) fractions (data not shown).

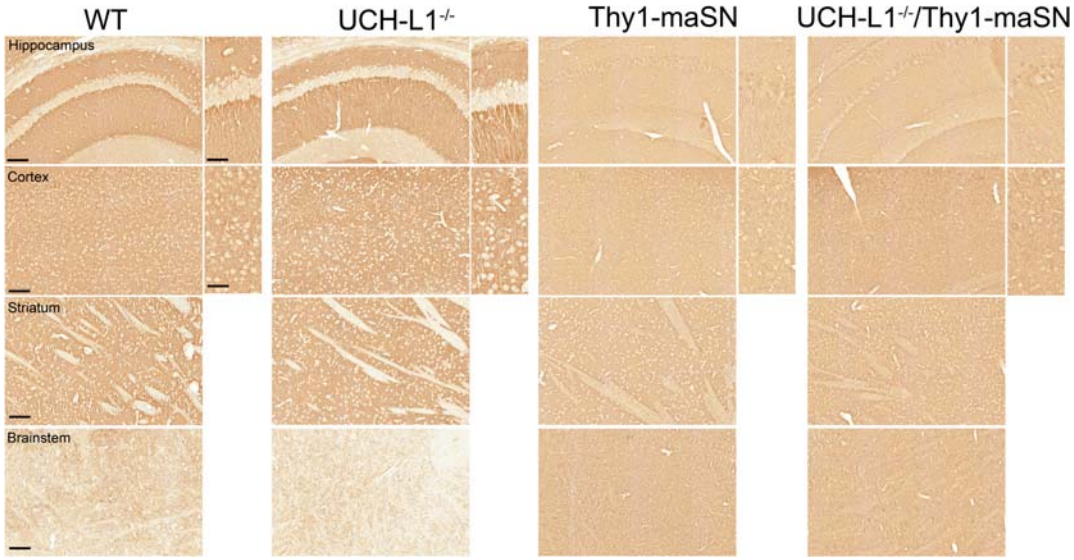

Figure 2 | αSN staining in UCH-L1$^{-/-}$/Thy1-maSN double as compared to Thy1-maSN single transgenic mice. Paraffin-embedded sagittal brain slices were stained for αSN. Hippocampus, motor cortex, striatum and brainstem for wildtype (WT), UCH-L1$^{-/-}$, Thy1-maSN and UCH-L1$^{-/-}$/Thy1-maSN mice are displayed. Brain regions and genotypes are indicated. Age of the animals: 3.5 months. Scale bars: 100 μm and for higher magnification pictures 50 μm.

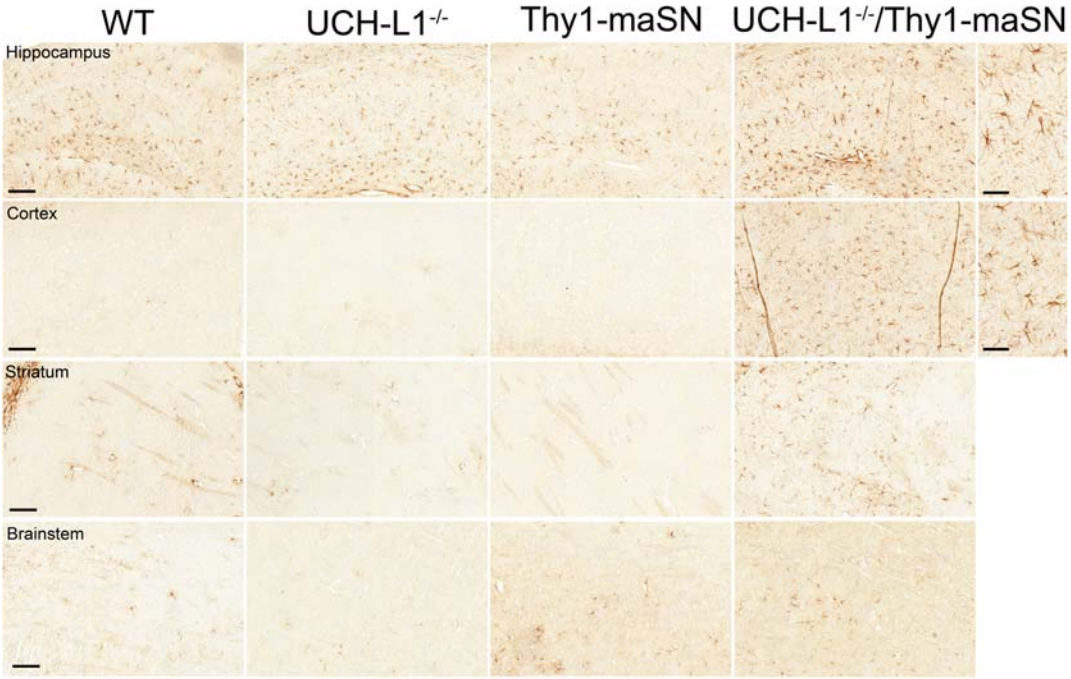

Figure 3 | Astrogliosis in 3.5-month-old UCH-L1$^{-/-}$/Thy1-maSN mutant mice. Paraffin-embedded sagittal brain slices were stained for GFAP. Hippocampus, motor cortex, striatum and brainstem for wildtype (WT), UCH-L1$^{-/-}$, Thy1-maSN and UCH-L1$^{-/-}$/Thy1-maSN mice are displayed. Brain regions and genotypes are indicated. Scale bars: 100 μm and for higher magnification pictures 50 μm.

In gad mice lacking UCH-L1, βSN and γSN but no αSN pathology has been reported[30] and these histopathological changes seem confined to the gracile nucleus in the brainstem. We analyzed γSN levels by Western blot in brainstem and forebrain extracts from UCH-L1$^{-/-}$ and double mutant mice but these proved similar (Figure 5) suggesting that the lack of UCH-L1 did not significantly affect αSN or γSN levels. For reference, the levels of endogenous huntingtin protein, which are regulated by proteasomal degradation, were also unaffected by UCH-L1 ablation (Figure 5).

Discussion

Collectively, our data show that UCH-L1-deficiency and excess murine wildtype αSN in mice act additively to aggravate disease. The disease process is accompanied by a massive astrogliosis in brain areas such as cortex, a phenomenon that is not seen in either of the single mutant mice. We found no evidence for UCH-L1-deficiency causing any significant changes in pathological αSN protein levels or species including S129-phosphorylated αSN and oligomers. Nor did we detect an earlier onset of immunohistopathological changes that are typically seen in end-stage αSN mice. It is therefore tempting to speculate that the observed disease-worsening effects occur by a mechanism that involves excess αSN exacerbating UCH-L1 deficiency and not *vice versa*. A perhaps provocative idea that will need further experimental support is that excess αSN may compromise UCH-L1 activity as part of αSN's pathophysiological effects in central and peripheral synapses.

UCH-L1 is widely expressed in brain and an abundant neuronal enzyme associated with several neurodegenerative diseases and cancer[17,18]. UCH-L1 protein is also found in neuronal inclusions of human PD and DLB brains[23], which perhaps in part explains the decreases in UCH-L1 activity that have been observed in such brain tissue[38,39]. UCH-L1 belongs to a family of enzymes that disassembles polyubiquitin chains to increase availability of free monomeric ubiquitin[19,44]. In addition to its hydrolase activity, UCH-L1 has been shown to have a dimerization-dependent ubiquityl ligase activity[21]. This latter activity was proposed to be in part pathogenic by causing an accumulation of αSN-ubiquitin conjugates and inhibiting αSN degradation, perhaps impairing also ubiquitin-proteasome activity[21]. Scenarios independent of UCH-L1 that impair ubiquitin-proteasome activity have also been postulated to explain αSN accumulation and the formation of Lewy inclusions in PD and other α-synucleinopathies[45–47].

In gad mice, loss of UCH-L1 leads to βSN and γSN pathology in specific brain nuclei and it gives rise to a dramatic phenotype that includes sensory ataxia, motor paresis and eventually premature death[29,30,48]. αSN pathology, however, has not been detected in gad and other UCH-L1-deficient mice. The observed increase in βSN in gad mice has been proposed as one possible explanation why αSN fails to accumulate in these mice because others have shown that βSN can counteract αSN aggregation[49]. Alternatively, UCH-L1 deficiency itself might suppress αSN aggregation.

Excessive amounts of murine wildtype αSN likely challenge the ubiquitin-proteasome protein-degradation machinery. UCH-L1 deficiency may compromise this system even further although direct evidence is lacking that the catalytic activity of the proteasome *per se* is significantly reduced when UCH-L1 is decreased[50]. On the other hand, UCH-L1 deficiency does reduce ubiquitin levels in the nervous system and this is accompanied by an up-regulation of lysosomal components. Therefore, Walters and colleagues put forward the hypothesis that UCH-L1 deficiency might affect a pool of ubiquitin that is utilized for lysosomal trafficking[31]. It is tempting to speculate whether excess αSN further compromises a lysosomal route in UCH-L1 mice because synuclein can not only impair chaperone-mediated autophagy but the protein itself seems to undergo intra-lysosomal degradation involving cathepsin D[51]. Further evidence is needed to strengthen or refute such a mechanism. Finally, we can not fully rule out the possibility that excess αSN and UCH-L1 deficiency act via two entirely independent pathways acting nonetheless additively to worsen disease.

Functional abnormalities in double mutants (earlier-onset motor deficits and increased muscle weakness) were already obvious at the age of 2.5 months but did not occur in mice that either over-express murine αSN in a wildtype UCH-L1 background or lack UCH-L1 but had wildtype αSN levels. At the age of 3.5 months, double mutants displayed one major histopathological change pointing at specific

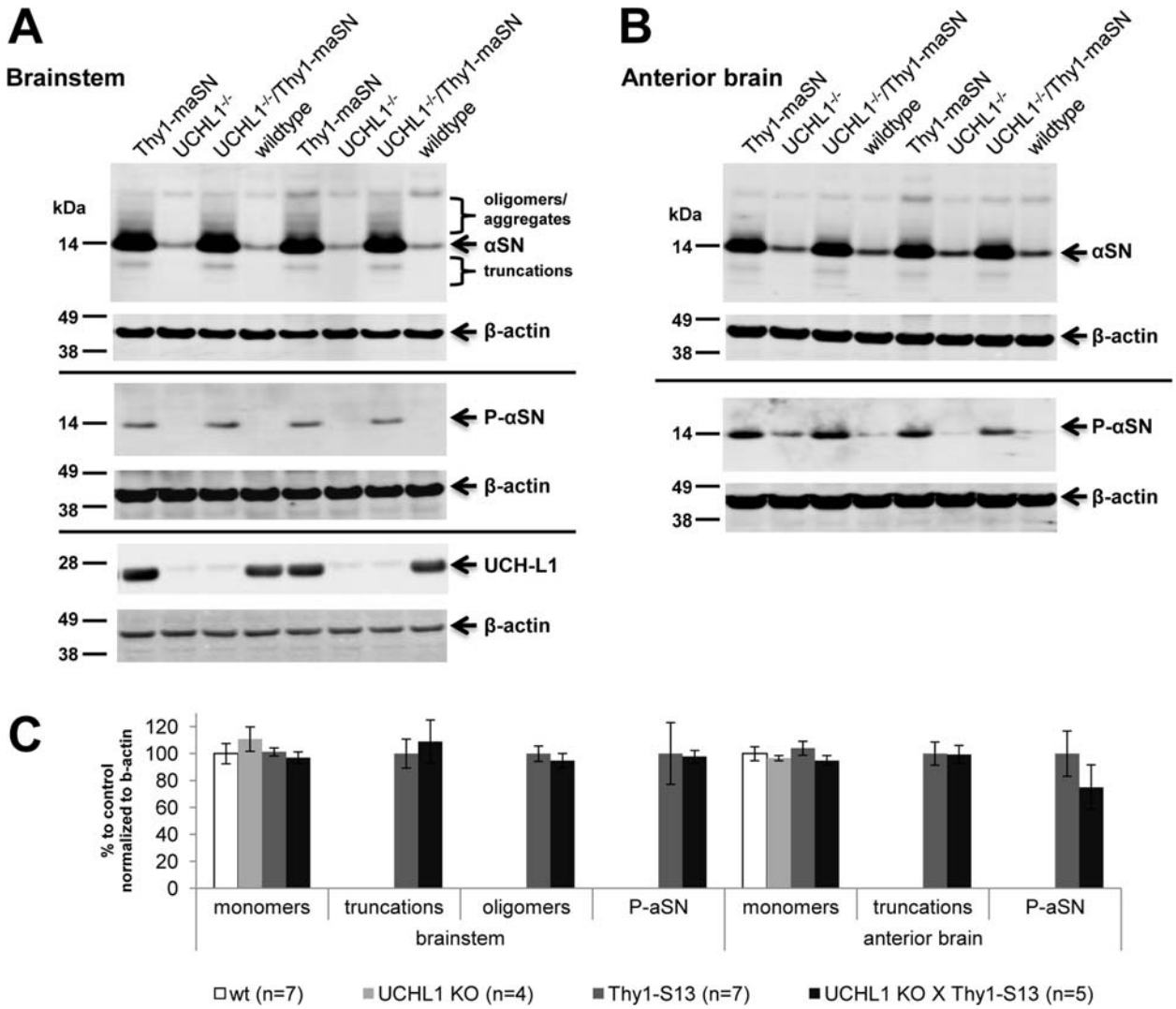

Figure 4 | Brain soluble αSN forms in UCH-L1$^{-/-}$/Thy1-maSN and Thy1-maSN mice. (A) Immunoblot analysis of brainstem extracts (supernatant/soluble fraction) from wildtype, UCH-L1$^{-/-}$, Thy1-maSN and UCH-L1$^{-/-}$/Thy1-maSN mice detecting αSN, S129-phosphorylated αSN and UCH-L1. β-actin was used as loading control. Indicated are the oligomers and truncations in mice over-expressing murine αSN. (B) Immunoblot analysis of anterior brain extracts (supernatant/soluble fraction) from wildtype, UCH-L1$^{-/-}$, Thy1-maSN and UCH-L1$^{-/-}$/Thy1-maSN mice detecting αSN and S129-phosphorylated αSN. β-actin is used for loading control. (C) Bar graph depicting quantification of the immunoblots shown in A. and B. for the different αSN species. See colour code for the different genotypes. Age of the animals: 3.5 months. N numbers for each genotype are indicated. Statsitical analysis: two-tailed, unequal variances Student's t-test.

disease-associated changes: a massive astrogliosis restricted to forebrain areas including cortex, hippocampus and striatum. Neurons in these brain areas express high levels of the αSN transgene but nonetheless remain largely devoid of hallmark histopathological cellular changes such as synuclein and ubiquitin pathology and axonal degeneration seen in brainstem and spinal neurons of end-stage Thy1-mαSN mice[41]. Interestingly, the brainstem in our double mutants showed no astrogliosis or microgliosis unlike in end-stage Thy1-mαSN mice. Why the forebrain-selective astrogliosis occurs in the double mutants is currently unknown. αSN seems to play a key role in the maintenance of SNARE-complex assembly and vesicle turnover in presynaptic terminals[52–54] and it seems likely that excessive amounts of αSN can perturb synaptic function that might trigger adaptive changes in astrocytes[55,56]. Astrogliosis is for example detected in mice showing enhanced synaptic excitability because of an editing-deficient GluR-B (GluA2) glutamate receptor subunit[57]. The combination of excess αSN together with UCH-L1 deficiency, which by itself is known to cause defects in central and peripheral synapses, perhaps suffices to pass a synaptic insult threshold that triggers astrocyte activation. Why this would occur mainly in forebrain and not in brain areas that otherwise seems most sensitive to αSN-induced pathology such as brainstem remains speculative. UCH-L1 is strongly expressed in both forebrain and brainstem[48,58]. Perhaps forebrain neurons are more responsive to a loss of UCH-L1 when αSN is in excess. UCH-L1 inhibition is known to preferentially affect the stability of certain synaptic proteins and their role is perhaps more relevant to forebrain neurons[50]. On the other hand, forebrain neurons seem normally quite capable of coping with an excess of αSN because in Thy1-mαSN mice, cortical and hippocampal neurons lack the dramatic histopathological changes seen in brainstem and spinal cord neurons. Possibly, forebrain neurons can better call upon compensatory mechanisms that reduce synaptic damage that at the same time trigger astrogliosis which might serve a neuroprotective role[59,60]. To conclude, further experiments are needed to better understand if and what kind of molecular interplay between αSN and UCH-L1 underlies the disease-worsening effect seen in double

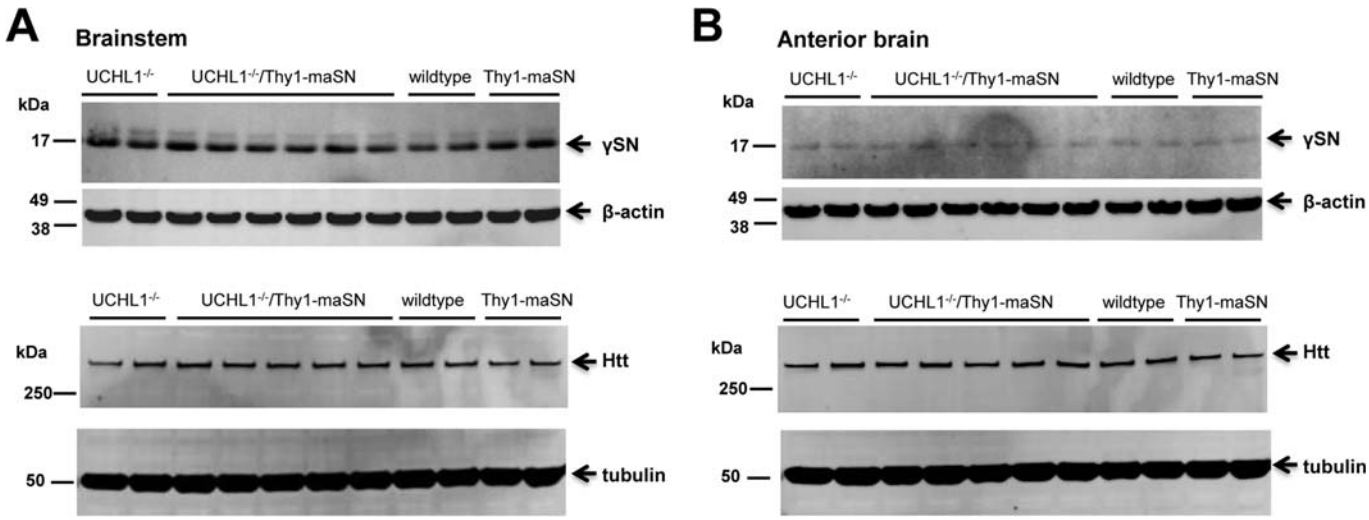

Figure 5 | γSN and huntingtin levels in the UCH-L1$^{-/-}$/Thy1-maSN mouse brain. (A) Immunoblot analysis of brainstem extracts from wildtype, UCH-L1$^{-/-}$, Thy1-maSN and UCH-L1$^{-/-}$/Thy1-maSN mice detecting soluble γSN. (B) Immunoblot analysis of anterior brain extracts from wildtype, UCH-L1$^{-/-}$, Thy1-maSN and UCH-L1$^{-/-}$/Thy1-maSN mice detecting soluble huntingtin (Htt). β-actin and tubulin were used as loading controls. Age of the animals: 3.5 months.

mutants as our data do not support a clear role for UCH-L1 in regulating monomeric, oligomeric, truncated and phosphorylated αSN levels. In addition, it has been reported that no alterations of dopaminergic cell loss in the absence of UCH-L1 in a viral α-synucleinopathy model could be observed[33]. We can of course not exclude that compensatory changes in UCH-L1 deficient mice such as the reported upregulation of lysosomal enzyme activities including cathepsin D[31], mask a role for UCH-L1 in the clearance of αSN. Future experiments using conditional UCH-L1 knockouts and/or determining whether perhaps more subtle effects can be detected in Thy1-maSN mice treated with UCH-L1 inhibitors or lacking only one UCH-L1 allele seem worth pursuing.

Methods

Statement on Animal Health. All experiments were carried out in accordance with authorization guidelines of the Swiss Federal and Cantonal veterinary offices for care and use of laboratory animals. Studies described in this report were approved by the Swiss Cantonal veterinary office and performed according to Novartis animal licence number 2063.

Transgenic mice. Thy1-maSN mice were generated and genotyped as described[41]. αSN knockout mice were obtained from Jackson laboratory (JolaHSD) and were kept as a homozygous line. UCH-L1 knockout (complete name: T1320UCHL1) mice were obtained form Deltagen (San Mateo, CA). Genotyping was performed with standard PCR protocol with the following primers: Oligo 56474 (5′-CTCTCCCCAGACTTAAGCTGCTTTG-3′) and Oligo 3196 (5′-GGGTGGGATTAGATAAATGCCTGCTCT-3′), expected band size of the targeted allele: 496 bp. Oligo 67696 (5′-CCTTGCCTCCGTCCTCTATTAAAGC-3′) and Oligo 56474, expected band size of the endogenous allele: 219 bp. All animals are kept in the C57BL/6 background and littermates were used as controls.

Immunoblot analysis. For infrared Licor western blot analysis brains were homogenized in homogenization buffer (10 v/w; 0.25 M Sucrose, 20 mM Tris 20 mM pH 7.4, 1 mM EDTA, 1 mM EGTA, 0.5 mM PMSF, 5 μg/mL Pepstatin A, 5 μg/mL Leupeptin, 1 : 1000 Okadaic acid 100 ng/μl in ethanol, 1 : 1000 Calyculin A 100 ng/μl in ethanol, 1 : 100 Pierce phosphatase inhibitor cocktail) with Precellys24 (Bertin Technologies, Rotation speed 5000 rpm, number of cycles: 2×30 sec, pause: 10 sec), then incubated for 30 min on ice and subsequently centrifuged at 13 krpm at 4°C for 20 min. Supernatant was used and protein concentration was determined by Bradford (Bio-Rad). 10 μg protein was loaded (LDS Sample Buffer, Sample Reducing Agent (Invitrogen), heated for 10 min at 95°C) on NUPAGE 4–12% Bis-tris gel 1.0 mm (Invitrogen) and ran at 180 V for 40–50 min with NuPAGE MES SDS Running Buffer (Invitrogen). Gels were blotted by semi wet transfer (Invitrogen X Cell II Blot Module) with NuPAGE Transfer Buffer, 20% methanol on invitrolon PVDF membrane (Invitrogen) at constant 30 V for 1 h. After transfer proteins were fixed on membrane (1 min in PBS full power in microwave). For Licor Odyssee detection membrane was blocked for 1 hr at room temperature in Odyssey Blocking Buffer (Odyssey, 1 : 1 diluted with PBS). Primary Antibodies (anti-phosphorylated α-synuclein, WAKO, 1 : 5000; mouse anti-α-synuclein, BD Transduction Laboratories, 1 : 5000; mouse anti β-actin, SIGMA, 1 : 15000; mouse anti-tubulin, AA13, abcam, 1 : 1000; rabbit anti-UCH-L1, #3524, Cell Signaling, 1 : 1000; rabbit anti-GFAP, Sigma, G9269, 1 : 500; mouse anti-Huntingtin, 2B7, 1 μg/ml; rabbit anti-γ-synuclein, #158, 1 : 1000) in Odyssey Blocking Buffer (0.2% Tween20). Membranes were washed 4 times for 5 min at room temperature in PBS containing 0.1% Tween20 and then incubated for 45 min (light protected) with secondary antibodies (Alexa Fluor 680, F(ab`)2 fragment of goat anti-mouse 2 mg/mL, 1 : 5000; IRDye 800CW anti-rabbit IgG, LI-COR, 1 : 5000) in Odyssey Blocking Buffer. Membranes were again washed 4 times for 5 min at roomtemperature in PBS containing 0.1% Tween20, then washed 2 times for 10 min at room temperature in PBS only and finally scanned and quantified on the Odyssey LI-COR System.

Immunohistochemistry. PBS-perfused brains were postfixed overnight in 4% formalin in PBS at 4°C. Then, the brains were dehydrated by different ethanol treatments using a Tissue-Tek VIP system (GMI Inc). The ethanol treatment series consisted of 70%, 80%, 90%, 2×94%, 3×100% ethanol each for 1 h. Brains were then washed 2 times in xylol for 30 min followed by 2 times in paraffin (30 min, 60 min). Subsequent, the dehydrated brains were embedded at 55°C in paraffin using a Tissue Block System TBS 88 (Geneq Inc). Slices were cut on a Microm HM 355 device (Microm International GmbH) at a thickness of 4–5 μm and mounted on superfrost glass slides (Microm International GmbH) and air-dried. Slides were kept at room temperature until use.

Immunohistochemistry was performed as following: Slides were incubated 3×10 min in day-1 buffer (0.01 M PBS, 1% BSA, 0.3% Triton X-100) and blocked by addition of 4% normal goat serum for 20 min. Paraffin-embedded slides were incubated in day-1 buffer with 1% normal goat serum and subsequently incubated overnight with a mouse monoclonal αSN antibody (1 : 800, 4B12, Abcam) and rabbit polyclonal anti-IBA1 (1 : 2000, Wako), anti-GFAP (1 : 2000, Z0334, Dako) and anti-ubiquitin (1 : 200, Z458, Dako) in a humidity chamber at room temperature. Slides were then rinsed 3×10 min in day-2 buffer (day-1 buffer diluted 1 : 3 in 0.01 M PBS). Slides were incubated for 1 h with secondary antibody (Biotin-conjugated goat anti-mouse IgG (1 : 200, Vectorlabs) and then with ABC reagent (Vectorlabs) for 1 h at room temperature. Slides were then rinsed in day-2 buffer 2×10 min, in 0.01 M PBS 2×20 min and were then desalted in 0.01 M Tris (pH 7.8). Slides were air-dried at room temperature and coversliped with eukitt mounting medium and analysed on a Nikon microscope.

Forelimb grip strength and rotating beam. To measure forelimb grip strength, mice are allowed to grasp a handle connected to a force-measuring device (San Diego Instruments, USA) and then pulled back with their tails until they release the handle. The best out of four consecutive trials is evaluated.

To measure motor coordination mice were placed on a rotating beam. The rotating beam was build in-house and is connected to a rotarod (Lugo Basile). It consists of a metal beam (Ø 1 cm, length 122 cm) coated with rubber attached to a rotarod (gradient angle upwards of 10°) which controls the constant rotating speed (4 rpm and 8 rpm). The beam is divided into four equal sections which are used for scoring the performance of the mice on the rotating beam (scores 1–5). The mouse is placed at the beginning on the already rotating beam facing upwards. If the mouse reaches the end of the beam without falling down or being head first hanging on the beam it gets a score of 1, if it falls down or is head first hanging in the last section (4th) it scores a 2, in

the 3rd section 3, in the 2nd section 4 and in the 1st section a score of 5. There is no time limit as the mice readily go upwards the rotating beam. One session consist out of two trials of 4 rpm and two trials of 8 rpm (all trials were included in the measurements), whereas the sequence is one trial of 4 rpm followed by on trial of 8 rpm in the morning and in the afternoon.

Maintenance. The animals were housed in a temperature-controlled room that was maintained on a 12 h light/dark cycle. Food and water were available *ad libitum*.

1. Esposito, E., Di Matteo, V. & Di Giovanni, G. Death in the substantia nigra: a motor tragedy. *Expert Rev Neurother* **7**, 677–697 (2007).
2. Dev, K. K., Hofele, K., Barbieri, S., Buchman, V. L. & van der Putten, H. Part II: alpha-synuclein and its molecular pathophysiological role in neurodegenerative disease. *Neuropharmacology* **45**, 14–44 (2003).
3. Vanderhaeghen, J. J., Perier, O. & Sternon, J. E. Pathological findings in idiopathic orthostatic hypotension. Its relationship with Parkinson's disease. *Arch Neurol* **22**, 207–214 (1970).
4. Bennett, M. C. The role of alpha-synuclein in neurodegenerative diseases. *Pharmacol Ther* **105**, 311–331 (2005).
5. Spillantini, M. G. *et al.* Alpha-synuclein in Lewy bodies. *Nature* **388**, 839–840 (1997).
6. Takeda, A. *et al.* Abnormal accumulation of NACP/alpha-synuclein in neurodegenerative disorders. *Am J Pathol* **152**, 367–372 (1998).
7. Wakabayashi, K., Matsumoto, K., Takayama, K., Yoshimoto, M. & Takahashi, H. NACP, a presynaptic protein, immunoreactivity in Lewy bodies in Parkinson's disease. *Neurosci Lett* **239**, 45–48 (1997).
8. Kruger, R. *et al.* Ala30Pro mutation in the gene encoding alpha-synuclein in Parkinson's disease. *Nat Genet* **18**, 106–108 (1998).
9. Polymeropoulos, M. H. *et al.* Mutation in the alpha-synuclein gene identified in families with Parkinson's disease. *Science* **276**, 2045–2047 (1997).
10. Singleton, A. B. *et al.* alpha-Synuclein locus triplication causes Parkinson's disease. *Science* **302**, 841 (2003).
11. Zarranz, J. J. *et al.* The new mutation, E46K, of alpha-synuclein causes Parkinson and Lewy body dementia. *Ann Neurol* **55**, 164–173 (2004).
12. Feany, M. B. & Bender, W. W. A Drosophila model of Parkinson's disease. *Nature* **404**, 394–398 (2000).
13. Kirik, D. *et al.* Nigrostriatal alpha-synucleinopathy induced by viral vector-mediated overexpression of human alpha-synuclein: a new primate model of Parkinson's disease. *Proc Natl Acad Sci U S A* **100**, 2884–2889 (2003).
14. Lee, M. K. *et al.* Human alpha-synuclein-harboring familial Parkinson's disease-linked Ala-53 --> Thr mutation causes neurodegenerative disease with alpha-synuclein aggregation in transgenic mice. *Proc Natl Acad Sci U S A* **99**, 8968–8973 (2002).
15. Masliah, E. *et al.* Dopaminergic loss and inclusion body formation in alpha-synuclein mice: implications for neurodegenerative disorders. *Science* **287**, 1265–1269 (2000).
16. van der Putten, H. *et al.* Neuropathology in mice expressing human alpha-synuclein. *J Neurosci* **20**, 6021–6029 (2000).
17. Ardley, H. C. & Robinson, P. A. The role of ubiquitin-protein ligases in neurodegenerative disease. *Neurodegener Dis* **1**, 71–87 (2004).
18. Yamazaki, T. *et al.* PGP9.5 as a marker for invasive colorectal cancer. *Clin Cancer Res* **8**, 192–195 (2002).
19. Larsen, C. N., Price, J. S. & Wilkinson, K. D. Substrate binding and catalysis by ubiquitin C-terminal hydrolases: identification of two active site residues. *Biochemistry* **35**, 6735–6744 (1996).
20. Wilkinson, K. D. *et al.* The neuron-specific protein PGP 9.5 is a ubiquitin carboxyl-terminal hydrolase. *Science* **246**, 670–673 (1989).
21. Liu, Y., Fallon, L., Lashuel, H. A., Liu, Z. & Lansbury, P. T., Jr. The UCH-L1 gene encodes two opposing enzymatic activities that affect alpha-synuclein degradation and Parkinson's disease susceptibility. *Cell* **111**, 209–218 (2002).
22. Osaka, H. *et al.* Ubiquitin carboxy-terminal hydrolase L1 binds to and stabilizes monoubiquitin in neuron. *Hum Mol Genet* **12**, 1945–1958 (2003).
23. Lowe, J., McDermott, H., Landon, M., Mayer, R. J. & Wilkinson, K. D. Ubiquitin carboxyl-terminal hydrolase (PGP 9.5) is selectively present in ubiquitinated inclusion bodies characteristic of human neurodegenerative diseases. *J Pathol* **161**, 153–160 (1990).
24. Leroy, E. *et al.* The ubiquitin pathway in Parkinson's disease. *Nature* **395**, 451–452 (1998).
25. Healy, D. G. *et al.* UCHL-1 is not a Parkinson's disease susceptibility gene. *Ann Neurol* **59**, 627–633 (2006).
26. Maraganore, D. M. *et al.* UCHL1 is a Parkinson's disease susceptibility gene. *Ann Neurol* **55**, 512–521 (2004).
27. Satoh, J. & Kuroda, Y. A polymorphic variation of serine to tyrosine at codon 18 in the ubiquitin C-terminal hydrolase-L1 gene is associated with a reduced risk of sporadic Parkinson's disease in a Japanese population. *J Neurol Sci* **189**, 113–117 (2001).
28. Ichihara, N. *et al.* Axonal degeneration promotes abnormal accumulation of amyloid beta-protein in ascending gracile tract of gracile axonal dystrophy (GAD) mouse. *Brain Res* **695**, 173–178 (1995).
29. Saigoh, K. *et al.* Intragenic deletion in the gene encoding ubiquitin carboxy-terminal hydrolase in gad mice. *Nat Genet* **23**, 47–51 (1999).
30. Wang, Y. L. *et al.* Accumulation of beta- and gamma-synucleins in the ubiquitin carboxyl-terminal hydrolase L1-deficient gad mouse. *Brain Res* **1019**, 1–9 (2004).
31. Walters, B. J. *et al.* Differential effects of Usp14 and Uch-L1 on the ubiquitin proteasome system and synaptic activity. *Mol Cell Neurosci* **39**, 539–548 (2008).
32. Chen, F., Sugiura, Y., Myers, K. G., Liu, Y. & Lin, W. Ubiquitin carboxyl-terminal hydrolase L1 is required for maintaining the structure and function of the neuromuscular junction. *Proc Natl Acad Sci U S A* **107**, 1636–1641.
33. Yasuda, T. *et al.* Effects of UCH-L1 on alpha-synuclein over-expression mouse model of Parkinson's disease. *J Neurochem* **108**, 932–944 (2009).
34. Kabuta, T., Furuta, A., Aoki, S., Furuta, K. & Wada, K. Aberrant interaction between Parkinson disease-associated mutant UCH-L1 and the lysosomal receptor for chaperone-mediated autophagy. *J Biol Chem* **283**, 23731–23738 (2008).
35. Setsuie, R. *et al.* Dopaminergic neuronal loss in transgenic mice expressing the Parkinson's disease-associated UCH-L1 I93M mutant. *Neurochem Int* **50**, 119–129 (2007).
36. Imai, Y., Soda, M. & Takahashi, R. Parkin suppresses unfolded protein stress-induced cell death through its E3 ubiquitin-protein ligase activity. *J Biol Chem* **275**, 35661–35664 (2000).
37. Sampathu, D. M., Giasson, B. I., Pawlyk, A. C., Trojanowski, J. Q. & Lee, V. M. Ubiquitination of alpha-synuclein is not required for formation of pathological inclusions in alpha-synucleinopathies. *Am J Pathol* **163**, 91–100 (2003).
38. Barrachina, M. *et al.* Reduced ubiquitin C-terminal hydrolase-1 expression levels in dementia with Lewy bodies. *Neurobiol Dis* **22**, 265–273 (2006).
39. Choi, J. *et al.* Oxidative modifications and down-regulation of ubiquitin carboxyl-terminal hydrolase L1 associated with idiopathic Parkinson's and Alzheimer's diseases. *J Biol Chem* **279**, 13256–13264 (2004).
40. Liu, Z. *et al.* Membrane-associated farnesylated UCH-L1 promotes alpha-synuclein neurotoxicity and is a therapeutic target for Parkinson's disease. *Proc Natl Acad Sci U S A* **106**, 4635–4640 (2009).
41. Rieker, C. *et al.* Neuropathology in mice expressing mouse alpha-synuclein. *PLoS One* **6**, e24834 (2011).
42. Yamazaki, K. *et al.* Gracile axonal dystrophy (GAD), a new neurological mutant in the mouse. *Proc Soc Exp Biol Med* **187**, 209–215 (1988).
43. Shimshek, D. R., Mueller, M., Wiessner, C., Schweizer, T. & van der Putten, P. H. The HSP70 molecular chaperone is not beneficial in a mouse model of alpha-synucleinopathy. *PLoS One* **5**, e10014.
44. Larsen, C. N., Krantz, B. A. & Wilkinson, K. D. Substrate specificity of deubiquitinating enzymes: ubiquitin C-terminal hydrolases. *Biochemistry* **37**, 3358–3368 (1998).
45. McNaught, K. S., Belizaire, R., Isacson, O., Jenner, P. & Olanow, C. W. Altered proteasomal function in sporadic Parkinson's disease. *Exp Neurol* **179**, 38–46 (2003).
46. McNaught, K. S. & Olanow, C. W. Proteolytic stress: a unifying concept for the etiopathogenesis of Parkinson's disease. *Ann Neurol* **53 Suppl 3**, S73–84; discussion S84–76 (2003).
47. Olanow, C. W. & McNaught, K. S. Ubiquitin-proteasome system and Parkinson's disease. *Mov Disord* **21**, 1806–1823 (2006).
48. Kurihara, L. J., Kikuchi, T., Wada, K. & Tilghman, S. M. Loss of Uch-L1 and Uch-L3 leads to neurodegeneration, posterior paralysis and dysphagia. *Hum Mol Genet* **10**, 1963–1970 (2001).
49. Hashimoto, M., Rockenstein, E., Mante, M., Mallory, M. & Masliah, E. beta-Synuclein inhibits alpha-synuclein aggregation: a possible role as an anti-parkinsonian factor. *Neuron* **32**, 213–223 (2001).
50. Cartier, A. E. *et al.* Regulation of synaptic structure by ubiquitin C-terminal hydrolase L1. *J Neurosci* **29**, 7857–7868 (2009).
51. Cullen, V. *et al.* Cathepsin D expression level affects alpha-synuclein processing, aggregation, and toxicity in vivo. *Mol Brain* **2**, 5 (2009).
52. Adamczyk, A. & Strosznajder, J. B. Alpha-synuclein potentiates Ca2+ influx through voltage-dependent Ca2+ channels. *Neuroreport* **17**, 1883–1886 (2006).
53. Liu, S. *et al.* alpha-Synuclein produces a long-lasting increase in neurotransmitter release. *Embo J* **23**, 4506–4516 (2004).
54. Chandra, S., Gallardo, G., Fernandez-Chacon, R., Schluter, O. M. & Sudhof, T. C. Alpha-synuclein cooperates with CSPalpha in preventing neurodegeneration. *Cell* **123**, 383–396 (2005).
55. Ballanyi, K., Grafe, P. & ten Bruggencate, G. Ion activities and potassium uptake mechanisms of glial cells in guinea-pig olfactory cortex slices. *J Physiol* **382**, 159–174 (1987).
56. Montgomery, D. L. Astrocytes: form, functions, and roles in disease. *Vet Pathol* **31**, 145–167 (1994).
57. Shimshek, D. R. *et al.* Forebrain-specific glutamate receptor B deletion impairs spatial memory but not hippocampal field long-term potentiation. *J Neurosci* **26**, 8428–8440 (2006).
58. Galter, D., Westerlund, M., Belin, A. C. & Olson, L. DJ-1 and UCH-L1 gene activity patterns in the brains of controls, Parkinson and schizophrenia patients and in rodents. *Physiol Behav* (2007).
59. Chen, Y. *et al.* Astrocytes protect neurons from nitric oxide toxicity by a glutathione-dependent mechanism. *J Neurochem* **77**, 1601–1610 (2001).

60. Saura, J. *et al*. Intranigral infusion of interleukin-1beta activates astrocytes and protects from subsequent 6-hydroxydopamine neurotoxicity. *J Neurochem* **85**, 651–661 (2003).

Acknowledgements

We wish to thank E. Regulier, C. Wiessner, P. Brebbia and K. H. Wiederhold for their support.

Authors contributions

DRS and PHvdP wrote the main manuscript text. DRS and PHvdP conceived and designed and DRS, TS and PS performed the experiments. DRS and TS prepared figures. All authors reviewed the manuscript.

Additional information

Supplementary information accompanies this paper at http://www.nature.com/scientificreports

Competing financial interests: The study was funded by the Novartis Pharma AG, who, through the employment of Derya R. Shimshek, Tatjana Schweizer, Peter Schmid and P. Herman van der Putten, had a role in conceiving, designing and performing the experiments and analyzing the data. There are no patents, products in development or marketed products to declare. This does not alter the authors adherence to all the *Scientific Reports* policies on sharing data and materials.

How to cite this article: Shimshek, D.R., Schweizer, T., Schmid, P. & van der Putten, P.H. Excess α-synuclein worsens disease in mice lacking ubiquitin carboxy-terminal hydrolase L1. *Sci. Rep.* **2**, 262; DOI:10.1038/srep00262 (2012).